Influence of torso protective equipment on intracorporeal shock wave behavior

H. Seeber[1], S. Grobert[2], D. Krentel[3] and T. Hauer[2]

[1]*Helmut Schmidt University – University of the Federal Armed Forces Germany Holstenhofweg 85, 22043 Hamburg, Germany,*
seeberh@hsu-hh.de
[2]*Bundeswehr Hospital Berlin – Department II, General and Thoracic Surgery, Scharnhorststraße 13, 10115 Berlin, Germany,*
[3]*German Federal Institute for Materials Research and Testing (BAM) Division 2.1 – Safety of Energy Carriers, Unter den Eichen 87, 12205 Berlin, Germany.*

Abstract. In the field of explosive reactions, there is a type of explosive effect that lacks a sufficient database and reproducible experiments regarding biomechanics. It concerns the primary explosive effect. It is defined as pure shock wave of the explosion. The physical behavior of the shock wave when interacting with different types of tissue and, in particular, the subsequent transitions of the shock wave, have barely been investigated. The transition of the shock wave into other materials is the focus of the research

Therefore, the aim of the investigations is the development of a multidisciplinary method to investigate shock wave behavior in various generic tissue simulants under the most reproducible conditions possible with realistic loads in an experimental test series with short set-up times. An autoclave is used to generate the pressure waves. A simplified torso model consisting of ballistic gelatin is used as a simulant.

In this paper, the influence of protective equipment on the pressure load in the tissue simulant is investigated. For this purpose, consecutive test setups are used. First, the behavior of ballistic gelatin as a tissue simulant is investigated. Then, the simplified torso model is covered with typical combat clothing consisting of four layers. Afterwards a currently used UHMWPE ballistic protective plate is placed in front of the simplified torso model. Finally, the combat clothing and the protective plate are examined in combination. Three cast-in pressure sensors are used as measuring devices, as well as an acceleration sensor attached to the protective plate.

The experiments show that the maximum overpressure in a model protected by combat clothing and the protective plate can be reduced by 95%. However, the propagation speed of the shock wave within the simplified torso model increases from 1535.5 m/s to 2204.5 m/s. This shows that even protective equipment, which is not primarily intended to protect against blast, offers a significant reduction in the pressure load in the protected area. On the one hand it is caused by the media transition from air to PE and the resulting higher reflection of the acceleration of the transmitted wave within the simulant. On the other hand, it is also reduced due to the damping and dispersion caused by the clothing layers.

1. Introduction

Blast injuries are among the most common injuries in military operations. Also, in civilian environments, more explosive threats are expected in the future due to emerging conflicts. While the effect of fragments, which is classified as secondary blast injury, could be minimized by police and military personnel's ballistic body protection systems, the effects of shock wave propagation in the body as part of the primary explosion trauma still remain a serious threat needing further research. Especially the highly dynamic pressure changes in the human body represent an area that has barely been investigated yet [1]. Dynamic pressure changes represent a relevant effect due to the reflection-related amplification of shock waves at organ-dermis interfaces and the compression and relief of the pressure wave at medium interfaces [2]. Various approaches have been used to investigate these aspects, like animal experiments on free field test sites or shock tube setups. Animal experiments have the disadvantage that measured values are interpreted with partly outdated or not validated limit values for overpressures (e.g. [3]). Whereas shock tube setups have limitations such as reflections, superimpositions, useable space and blocking [4]. Injury mechanisms and their effects have not yet been sufficiently elucidated for the torso and extremities [2].

Therefore, the intention is to use an experimental setup that allows for the generation of reproducible pressure waves under free-field conditions and the application of those waves to a sufficiently large body model. In a broader sense, the influence of combat clothing and personal protective equipment on the shock wave behavior of different tissue types is correspondingly less studied [5]. Therefore, this paper focuses on the behavior of the shock wave in a simplified first stage torso model after it has passed through personal protective equipment.

The paper is structured as follows. First, the experimental setup and materials, such as the simplified torso model, the protective plate and the clothing layers are introduced. Afterwards, the

measurement results are presented. Especially the pressure values in the torso model are considered. It concludes with a discussion of the results and an outlook of the further work.

2. Materials and Methods

2.1 Experimental Setup

The experimental setup used is shown in Figure 1 as a schematic illustration with distance specifications, as well as an overall view. In the following, the components of the experimental setup are explained related to the schematic illustration. The pressure wave is generated by a cylindrical autoclave, further called shock wave generator (SWG) (A). It has a volume of 0.065 m^3. It is filled with a stoichiometric acetylene-oxygen mixture under atmospheric conditions. Ignition takes place through an electronic detonator. The pressure wave escapes through a 12.5 cm diameter outlet, which is covered by an aluminum burst disc. The center of the outlet is 1.35 m above ground. Preliminary tests showed that the pressure wave propagates in a hemispherical shape. The simplified torso model (STM) is described in more detail in Section 2.2.1. (B). A high-speed camera is used to document the pressure wave propagation (C). The specification of the protective plate is described in Section 2.2.2. (D). The arrangement of the clothing layers is explained in Section 2.2.3. (E). The pencil probes (1, 4) are used to record the pressure values of the pressure wave in front of the STM. In addition, a runtime determination can be carried out. Kistler 6233AA0025 sensors are used for this purpose. Positions 6 - 8 are piezoelectric pressure sensors (three times PCB 132B38) casted into the STM. The orientation is side-on. The exact positioning is described in Section 2.2.1. Position 9 is an accelerometer (PCB 356A01), which is directly applied to the protective plate. The exact positioning can be found in Section 2.2.2. In general, a sample rate of 2 MHz is used.

Figure 1. Left side: schematic setup. A: shock wave generator; B: simplified torso model; C: high-speed camera; D: protective plate; E: clothing; 1, 4: pencil probes; 6 - 8: internal pressure sensors, 9: accelerometer. Right side: measurement setup as an overview photo.

2.2 Materials

2.2.1 Simplified Torso Model

The simplified torso model (STM) consists of 17% (w/v) ballistic gelatin. Gelatin is produced according to the common procedures [6]. The used gelatin has a gel strength of 265 bloom. The mixing ratio of 17 w% is chosen based on measurements of the internal sound velocities. Ultrasonic transit time measurements are used to measure the internal sound velocity of gelatin samples with different mixing ratios. Human soft tissue, consisting of muscle and fat, is taken as the target value for the sound velocity. The individual sound velocities are calculated using their percentage distribution on the human body (limitations are known). For generic muscle tissue, a sound velocity of 1582.5 m/s and a distribution in the human body of 31.56 w% is chosen [7]. For fat tissue, a sound velocity of 1450 m/s and a distribution in the human body of 13.63 w% is chosen [7]. This leads to a calculated sound velocity for soft tissue of 1542.4 m/s. This value applies well to the calculated value of 17 w% gelatin. For the gelatin used in these experiments, an internal sound velocity of 1522 m/s is measured.

The body model is in a rectangular shape with dimensions of 40 x 23 x 27 cm. In this test series, one side of the block is provided as a negative mold, which fits the protective plates. This convex shape allows full contact of the STM front surface with the protective plate, without an air gap between them. The STM is placed on a tripod with a table. The model is held on the tripod only by its weight. It is equipped with three cast-in piezoelectric pressure sensors (PCB 132B38). The orientation of the sensor is side-on. A sketch showing the exact positioning of the pressure sensors and a detail photo of the instrumented STM is displayed in Figure 2.

Figure 2. Left side: Sketch of the instrumented simplified torso model. Middle: Detail view of instrumented body model with protective plate attached. Right side: Sketch of the instrumented protective plate.

2.2.2 Protective Plate

In these trials, the focus is on torso protective equipment. Therefore, a chest protection plate from a plate carrier currently used by an army is used. This plate fulfills the test standard of protection class 6 (7,62 mm x 39, Fe-Core) of the Association of Test Laboratories for Attack Resistant Materials and Constructions (VPAM) [8]. It uses an ultra-high molecular weight polyethylene (UHMWPE) material as hard ballistic. Due to the stand-alone feature of the VPAM 6 plate, it has an integrated shock absorber layer. The plate is shaped concave in the direction of loading. The outer dimensions are 24 by 32 cm and the thickness is 1.9 cm. In the upper area, the plate has a trapezoid shape (Figure 2 r.s.).

The protective plate was mechanically clamped with the STM only (Figure 2 mid.). The contact pressure was adjusted so that it was comparable to the real operational conditions when worn with a real vest. Despite the concave shape of the plates, they lay flat on the face of the STM, since this face was cast as a negative mold. The accelerometer is posed directly onto the plate back face (Figure 2 r.s.). The position is related to the center of the tripod plate. The height of the accelerometer is 19 cm and the distance from the side edge is 12 cm.

2.2.3 Combat Clothing

Combat clothing is added over the STM. The area of the back side faces in the direction of the shock wave generator. This allows the most even and uniform textile layers possible. The structure of the clothing layers and their materials are stated in Table 1. In these trials where the protective plate has been added, it is placed between the undercoat rain protection and combat jacket. The layers are loosely arranged against each other. There is no mechanical clamping of the clothing to the tripod.

3. Experimental method

In this section, the experimental system used is presented. Table 2 lists the experiments carried out. The overall objective is to determine the influence of the protective equipment on the shock wave in the simplified torso model. For this purpose, each configuration with the STM is first considered individually. The influence of the combinations can then be identified with these comparative values.

Table 1. Layered structure of the used clothing.

Layer	1	2	3	4
Type	t-shirt	undercoat cold protection	undercoat rain protection	combat jacket with flame protection
Material	polyester	polyester / polyamide	polyamide	viscose fiber / aramid
Picture				

Table 2. Experimental systematic.

No.	Description/Configuration	Section
1.5	Gelatin, individual	4.1
1.6		
1.11	Gelatin + Clothing	4.2
1.12		
1.7	Gelatin + Protective Plate	4.3
1.8		
1.13	Gelatin + Protective Plate + Clothing	4.4
1.14		
1.15		
1.16		

4. Results

In this section, the results of the tests are presented in a respective sub-section. Specifics of the test configurations are discussed directly.

4.1 Gelatin, individual

In this experiment, the simplified torso model (STM) is placed individually on the tripod plate. The measured values for the tests can be seen in Table 3. The corresponding graphs of the external and internal overpressure can be seen in Figure 3.

The curve of the internal overpressure shows the typical pressure curve. Three distinctive peaks can be seen in the pressure curve of the front sensor. The first peak is the incident peak. The second peak represents a reflection peak from the base plate and the third peak represents a reflection peak from the following sensor.

Table 3. Measured and calculated (italic) values at tests No. 1.5 and 1.6.

No. /Unit	Max. outside overpressure at 1 m	Impulse duration	Pressure wave propagation velocity (Avg.)	Max. inside overpressure at the front sensor	Shockwave propagation velocity (Avg.)
	[kPa]	[ms]	[m/s]	[kPa]	[m/s]
1.5	92,1	*0,84*	*450,1*	83,9	*1539,9*
1.6	82,4	*1,17*	*459,6*	88,7	*1533,7*
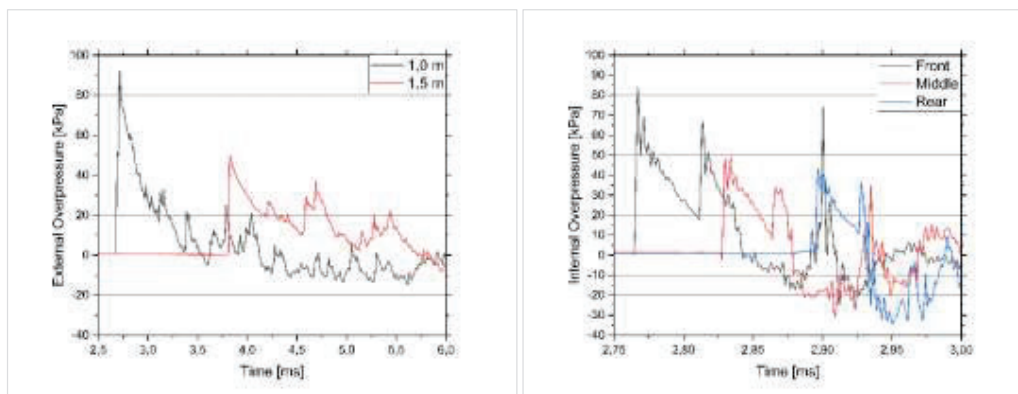
Figure 3. Left side: external overpressure. Right side: internal overpressure. (No.1.5)

4.2 Gelatin + Clothing

In this experiment, the STM is placed on the tripod plate. In addition, four layers of clothing are placed over the STM as shown in Table 1. The measured values for the test can be seen in Table 4. The corresponding diagrams of the external and internal overpressure can be seen in Figure 4 respectively in Figure 5. Due to the characteristic of the pressure curves, the runtime determination was not done by the peaks, but by the beginning of the pressure rise.

Table 4. Measured and calculated (italic) values at tests No. 1.11 and 1.12.

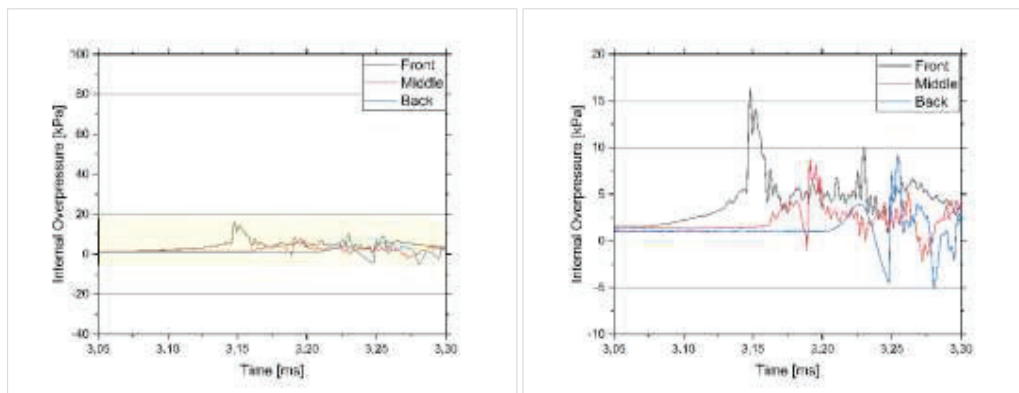| No. /Unit	Max. outside overpressure at 1 m	Impulse duration	Pressure wave propagation velocity (Avg.)	Max. inside overpressure at the front sensor	Shockwave propagation velocity (Avg.)
	[kPa]	[ms]	[m/s]	[kPa]	[m/s]
1.11	79,4	*1,19*	*471,5*	25,4	*1587,3*
1.12	71,8	*0,72*	*468,2*	15,1	*1587,3*
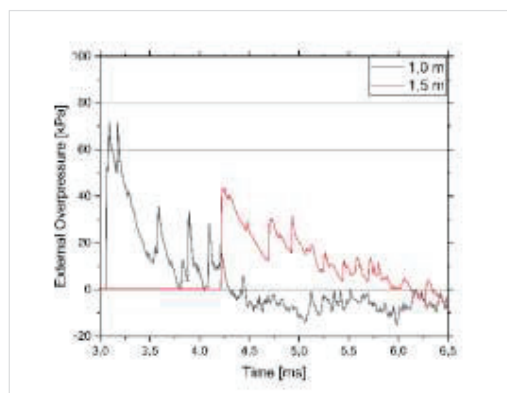
Figure 4. External overpressure (1.12).

158
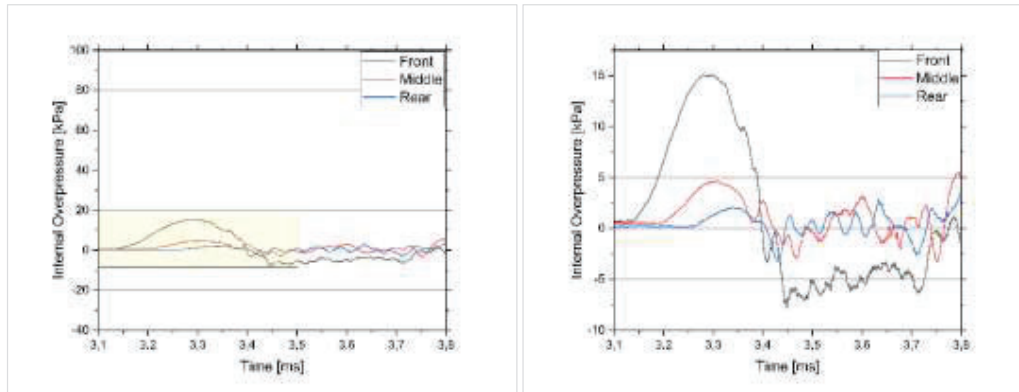
Figure 5. Left side: internal overpressure. Right side: internal overpressure, marked segment enlarged from the left graph. (1.12)

4.3 Gelatin + Protective Plate

In this experiment, the STM is placed on the tripod plate with a fastened protective plate in front of it. The measured values for the test can be seen in Table 5. The corresponding diagrams of internal overpressure can be seen in Figure 6 and of the acceleration in Figure 7.

With the measured acceleration values, there is a strong upswing of the entire STM starting at about 3.5 ms after ignition. The actual impact effect of the pressure wave takes place at 3.4 ms. Therefore, the 400 g acting at 3.4 ms are recorded. This time also correlates with the impact of the pressure wave on the pencil probe at 1 m distance. The swinging afterwards is caused by the free movement of the body model on the tripod plate. This does not represent an effect that can be found in real life.

Table 5. Measured and calculated (italic) values at tests No. 1.7 and 1.8.

No. /Unit	Max. outside overpressure at 1 m	Impulse duration	Pressure wave propagation velocity (Avg.)	Max. inside overpressure at the front sensor	Inside shockwave propagation velocity (Avg.)	Acceleration in propagation direction
	[kPa]	[ms]	[m/s]	[kPa]	[m/s]	[g]
1.7	95,6	*0,81*	*451,1*	16,3	*2325,6*	400
1.8	86,1	*0,99*	*468,2*	13,8	*2083,3*	371

Figure 6. Left side: internal overpressure. Right side: internal overpressure, marked segment enlarged from the left graph. (1.7)
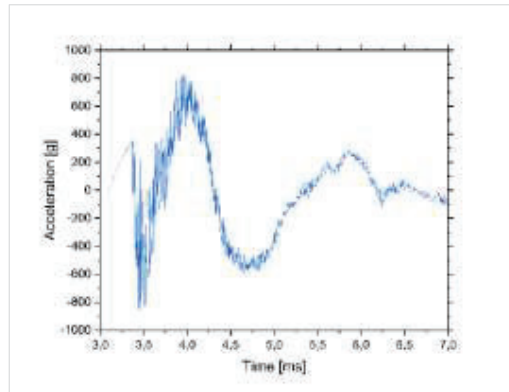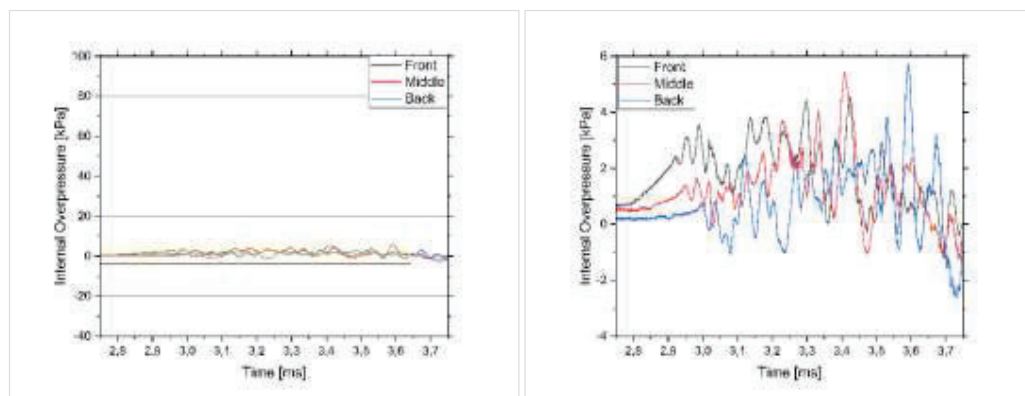
159

Figure 7. Acceleration (1.7).

4.4 Gelatin + Protective Plate + Clothing

In this experiment, the STM is placed on the tripod plate. It is covered with the clothing layers one to three (Table 1). Then the protective plate is fastened. Clothing layer four is then placed over it. For test numbers 1.13 and 1.14, the part of the clothing located under the tripod plate is fastened around the tripod. In test numbers 1.15 and 1.16, this part is freely movable. The measured values for the test can be seen in Table 6. The corresponding diagrams of internal overpressure can be seen in Figure 8 and of the acceleration in Figure 9.

It can be seen that lower accelerations are transferred to the STM in the tests where the clothing is fastened. A reason for this is the slap effect of the fourth cloth layer which can move freely in tests 1.15 and 1.16. Due to the characteristic of the pressure curves, the runtime determination was not done by the peaks, but by the beginning of the pressure rise. In test No. 1.15, the mean internal pressure sensor did not record any data, therefore a calculation of the internal propagation velocity was not possible. The error was due to a loose cable connection.

Table 6. Measured and calculated (italic) values at tests No. 1.13, 1.14, 1.15 and 1.16.

No. /Unit	Max. outside overpressure at 1 m	Impulse duration	Pressure wave propagation velocity (Avg.)	Max. inside overpressure at the front sensor	Shockwave propagation velocity (Avg.)	Acceleration in propagation direction
	[kPa]	[ms]	[m/s]	[kPa]	[m/s]	[g]
1.13	99,5	*0,68*	*461,9*	4,2	*1754,4*	364
1.14	89,1	*0,77*	*455,2*	3,5	*1904,8*	355
1.15	76,3	*0,71*	*474,4*	3,0	Def.	389
1.16	92,0	*1,25*	*457,7*	4,4	*1709,4*	422

Figure 8. Left side: internal overpressure. Right side: internal overpressure, marked segment enlarged from the left graph. (1.16)
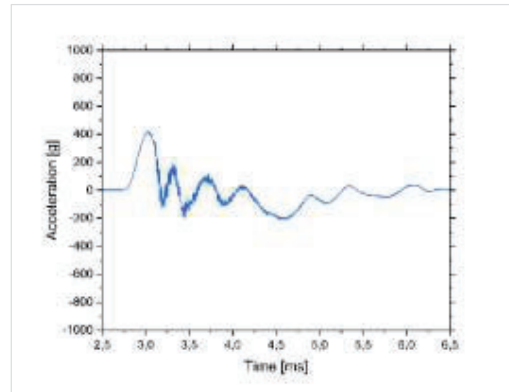
Figure 9. Acceleration (1.16).

5. Discussion

The external overpressure shows an ideal pressure curve (Figure 3 l.s.) [9]. A sudden increase followed by an almost exponential decrease in pressure. This is followed by the transition to negative overpressure and the leveling off around normal pressure. With optimum curve progression, 90 kPa overpressure is generated at a distance of 1 m in the test series. Lower maximum pressures (avg. 78 kPa) can be explained by a double peak at the maximum pressure peak (Figure 4). The impulse remained almost identical in both cases. On average, the impulse of the generated pressure wave is 37 kPa·s. The average impulse duration is 0.9 ms. Based on the time between the peaks of the pressure wave at the pencil probes at 1 m and 1.5 m distance, the average propagation velocity can be estimated. On average, the propagation velocity of the generated pressure wave is 458.72 m/s. Thus, the load case presented here remains below the level of a load case relevant for injury. It must of course be noted that there are no universal or validated injury thresholds [10]. However, the commonly used blast injury threshold curve of Bass et al. is used here as a guideline [3]. This results in a load case target value of 200 kPa at 2 ms duration. However, the characteristics of the pressure curve correspond to the expectations for a military explosive. The generated pressure wave can therefore be used for a general consideration of the effect of protective equipment on the internal shock wave, as it is a quantitative consideration.

For the internal pressures, it shows that through the clothing, the protective plate and then the combination of both, the pressure decreases (Table 7). Adding the plate and clothing reduces the maximum pressure to 5% of the pressure that occurs with an unprotected simplified torso model (STM). Furthermore, the respective protective equipment has an influence on the pressure curves and, thus, especially on the impulse. The adding of the clothing shows that the rapid increase in pressure is dampened. Almost bell curves are created (Figure 5). This shape of the curve, which almost corresponds to a mechanical excitation, is caused by the clothing layers, which act like a spring-damper system on the applied pressure wave. The respective maximum pressures are reduced. When the protective plate is added, very narrow peaks occur in the pressure curve (duration: 0,05 ms). These peaks show a rapid increase followed by a rapid decrease in pressure. The maximum pressure is lower. In both cases, the frequency of oscillation of the graph around normal pressure is lowered. So, one oscillation in the unprotected STM lasts 0.2 ms. In STM protected by clothing it lasts 0.7 ms. In the combination of clothing and a protective plate, the effects of both components occur in combination (Figure 8). The pressure sensors are not fully acceleration compensated inside the STM. Therefore, an acceleration of the sensors occurs, which is visible as oscillations of the pressure (< 1 kPa) (Figure 8).

Table 7. Avg. maximal internal overpressure at the first pressure sensor for every test configuration.

Configuration	Gelatin, indiv.	Gelatin + Clothing	Gelatin + Protective Plate	Gelatin + Protective Plate + Clothing
Internal peak overpressure (1st max.) (avg.) [kPa]	86,3	20,3	15,1	3,8

Comparing the propagation speed of the shock wave in the unprotected STM with that in the one protected by the protective plate, an increase in the propagation speed of 669 m/s (44%) can be observed. This can be explained by means of impedance estimation. The following equation is used to estimate the material flow velocity [11]:

$$u_B = u_A \frac{2Z_A}{Z_A + Z_B} \tag{1}$$

Where u is the material flow velocity, Z is the acoustic impedance, subscript A is the origin material and subscript B is the coupling material. The material flow velocity is directly proportional to the propagation velocity. Therefore, it can be seen that at the transition from air to UHMWPE material, there is compression of the pressure wave. At the transition from UHMWPE material to gelatin, a decompression occurs. The decompression of the shock wave explains the increased velocity of propagation and the reduced maximum pressure (Table 5). The clothing layers also lead to an acceleration of the shock wave by 3% (Table 4). In combination with the protective plate, the clothing leads to absorption, since the propagation velocities in the combined setup are lower than in the setup with the protective plate by itself.

Considering the influence of acceleration, it can be seen that it has a maximum value of 385.5 g on average. The curve corresponds to that of a mechanical excitation and can thus be expected (Figure 7). Therefore, this is the acceleration that is induced by the pressure wave to the equipment and consequently to the STM. An effect of the clothing over the protective plate is not noticeable, as the excitation affects the entire tripod.

6. Conclusion and Future Work

The aim of this paper is to show the effect of protective equipment on the transmission and behavior of a shock wave in a simplified torso model. In summary, the combination of a UHMWPE protective plate and combat clothing has an attenuating but accelerating effect on the shock wave. Thus, the maximum overpressure is reduced by 95%. The impulse of the shock wave is reduced by 63%. The propagation speed is increased from 1532.50 m/s to 2204.55 m/s by the UHMWPE protective plate. The shock wave generator produces 90 kPa at a distance of 1m with an impulse duration of 0.9 ms in the configuration used during these experiments.

Also, it is important to consider the limitation that, in this case, the simplified torso model is protected over the entire frontal exposed area, which in reality is only a small part of the body. Moreover, the current version of the STM represents only a highly simplified version, which can be used to show the shock wave behavior in a well recognizable way. In addition, the load case is specifically relevant to highly exposed personnel, such as tactical door breaching operators, who are repeatedly exposed to comparable low-level blast. No injury-mechanical effectiveness can be assigned to the load cases generated for the tests. The reason for this is that there are many variables (some of which are unknown) that influence the effectiveness of injury mechanisms [2]. Nevertheless, the observations can be applied qualitatively.

Future objective will be to investigate the simplified torso model by means of injury-relevant relevant load cases in order to be able to make quantitative statements. Furthermore, the media transition of the shock wave within the model will be in the focus. Solids (bone simulants), air inclusions (hollow organs) and gelatin of different densities will be integrated into the simplified torso model. The detection of the shock wave is mainly done by means of pressure sensors. In addition, a general installation of the accelerometer is to be considered.

References

[1] Callaway, D. W, Burstein, J. L., Operational and Medical Management of Explosive and Blast Incidents. (Springer International Publishing, Cham, 2020); pp.19 – 35.
[2] Bull A.M.J., Clasper, J., Mahoney, P. F, Blast Injury Science and Engineering (Springer International Publishing, Cham, 2016); pp. 71 – 84.
[3] Bass, C. R., Rafaels, K. A., Salzar, R. S., Pulmonary injury risk assessment for short-duration blasts, The Journal of trauma, 65, 2008; pp. 604 – 615.
[4] Needham C.E. et al., Blast Testing Issues and TBI: Experimental Models That Lead to Wrong Conclusions, Frontiers in neurology, 6, 2015, No. 72.

[5] Hattingh, T. S., Skews, B. W., Experimental investigation of the interaction of shock waves with textiles. Shock Waves 11, 2001; pp. 115-123.

[6] Sellier K., Bolliger S., Kneubuehl B. P., Wundballistik Und Ihre Ballistischen Grundlagen (Springer, Berlin / Heidelberg, 2013); pp. 178 – 196.

[7] Azhari H., Basics of biomedical ultrasound for engineers (Wiley, Hoboken, N.J, 2010); pp. 313 – 314.

[8] Association of Test Laboratories for Attack Resistant Materials and Constructions (VPAM), General Basics of Ballistic Material, Design and Product Tests (Test Guideline: 2021-03).

[9] Sochet, I., Blast Effects, Physical Properties of Shock Waves (Springer International Publishing, Cham, 2018); pp. 37 – 57.

[10] Boutillier J., et al., A critical literature review on primary blast thorax injury and their outcomes, The journal of trauma and acute care surgery, 81, 2016, 371 – 379.

[11] Cooper P., Explosives engineering (Wiley-VCH New York, Chichester, Weinheim, Brisbane, Singapore, Toronto, 1996); pp. 203 – 223.